

Equilibrium and nonequilibrium electron tunneling via discrete quantum states

Mandar M. Deshmukh, Edgar Bonet, A. N. Pasupathy, and D. C. Ralph
Laboratory of Atomic and Solid State Physics, Cornell University, Ithaca, New York 14853

(Received 1 June 2001; published 7 January 2002)

We analyze quantitatively the resonance energies, widths, and amplitudes for electron tunneling via the quantum levels of a metal nanoparticle. We consider both the regime where only one quantum state is accessible for tunneling and the nonequilibrium regime where additional states are made accessible one by one. For tunneling through one state, our results agree with expectations for sequential tunneling, but in the nonequilibrium regime the resonances are broadened and shift with temperature in ways that require taking into account electron interactions and relaxation.

DOI: 10.1103/PhysRevB.65.073301

PACS number(s): 73.22.-f, 73.23.Hk, 74.80.Bj

In nanometer-scale devices, electron tunneling can be used to probe the spectrum of discrete quantum states. By varying gate and source-drain voltages (V_g, V) in a transistor geometry, energy levels have been measured inside semiconductor quantum dots,¹ metal nanoparticles,² and molecules.³ Despite the popularity of this technique, little attention has been paid to the detailed quantitative form of the tunneling resonances, particularly, when measured as a function of increasing source-drain bias. Here, we analyze the energies, current amplitudes, and widths of individual tunneling resonances. By varying V_g and V , we can manipulate electron flow controllably through one state, or through many, and we can extract tunneling rates for each level. When only one state participates in tunneling, the resonance properties are in accord with expectations for simple sequential tunneling. However, for larger voltages, the resonance energies, widths, and currents can all be modified by the population of excited quantum states. For an understanding of the high- V regime, nonequilibrium transitions beyond those considered previously must be taken into account.

A cross-sectional device schematic is shown in Fig. 1(a). The use of an aluminum particle with aluminum oxide tunnel barriers provides mechanical and charge stability, and allows V and V_g to be varied without significantly altering barrier resistances. Fabrication⁴ is done using electron-beam lithography and reactive-ion etching to create a bowl-shaped hole in a silicon-nitride membrane, with a minimum diameter ~ 10 nm. A gate electrode is formed by depositing 18.5-nm Al, followed by anodization to 3.5 V in an oxygen plasma, and then deposition of 8.5 nm of SiO_x . The rest of the device is made by depositing a thick Al electrode onto the bowl-shaped side of the membrane, oxidizing for 3 min in 50 mTorr of O_2 , depositing 1.5-nm Al onto the other side of the device to make a layer of Al nanoparticles, oxidizing, and then depositing the lower Al electrode. Device parameters are determined from the large- V structure of the 4.2-K Coulomb staircase curve.⁵ The capacitance of nanoparticle to the top electrode is $C_L=7.9$ aF, to the bottom electrode $C_R=2.7$ aF, and the gate capacitance is $C_g=0.06$ aF. The sum of the resistances of the two tunnel junctions is $R_\Sigma \approx 3$ M Ω , with individual resistances sufficiently large that the intrinsic widths of the quantum states are smaller than $k_B T$. Assuming a roughly hemispherical particle shape,⁵ and a capacitance per unit area of 0.05 aF/nm² (Ref. 6), we es-

timate a nanoparticle diameter ~ 10 nm.

In Fig. 1(b), we plot the differential conductance dI/dV as a function of V_g and V , when the sample is cooled in a dilution refrigerator with copper-powder filters on the electrical leads. The lines in the figure are due to tunneling resonances through discrete quantum states in the nanoparticle. Lines having a positive slope correspond to tunneling thresholds across the lower-resistance junction L , and negative slopes are thresholds across junction R (Ref. 2). The discontinuity evident in the figure is due to a V_g -driven change in the charge on another nanoparticle adjacent to the one through which tunneling occurs. This merely shifts the electrostatic potential of the current-carrying particle. The intrinsic energies, current levels, and widths of the resonances are not otherwise altered, so that the full dI/dV spectrum can be constructed. From the absence of spin-Zeeman splitting in a magnetic field (not shown) for resonance lines I and II, we can identify these transitions with tunneling from an odd number of electrons n_0 on the particle to an even number.⁷ Since these resonances require increased $|V|$ as a function of V_g , they are $n_0 \rightarrow n_0 - 1$ transitions. (See Fig. 2.) Resonances III and IV correspond to even $(n_0 - 1) \rightarrow \text{odd } n_0$ transitions. The large gaps in V between each of resonances I and II and the next parallel lines are due to the energy difference $\sim 2\Delta$ between a fully paired superconducting state in the Al particle and the next lowest-energy tunneling state with two quasiparticles.⁴

Equilibrium regime. We first consider the region of V_g near -650 mV, where V_g and V can be adjusted so that a single spin-degenerate quantum state (state 0) is accessible for tunneling [I - V curves are shown in Fig. 1(c)]. For the case under consideration, in which the quantum level is either empty or singly occupied, the current predicted for sequential tunneling is⁸⁻¹¹

$$I = e \frac{2\gamma_{0L}\gamma_{0R}(f_L - f_R)}{(1+f_L)\gamma_{0L} + (1+f_R)\gamma_{0R}}, \quad (1)$$

where γ_{0L} (γ_{0R}) is the bare rate for an electron to tunnel from the quantum state 0 to an unoccupied density of states in electrode L (R) and f_i is the occupation probability for states in electrode i with energy equal to the resonance state (for a thermal distribution $f_i = \{1 + \exp[(\epsilon_0 - \mu_i)/kT]\}^{-1}$, with ϵ_0 the energy to occupy the quantum state, and μ_i the

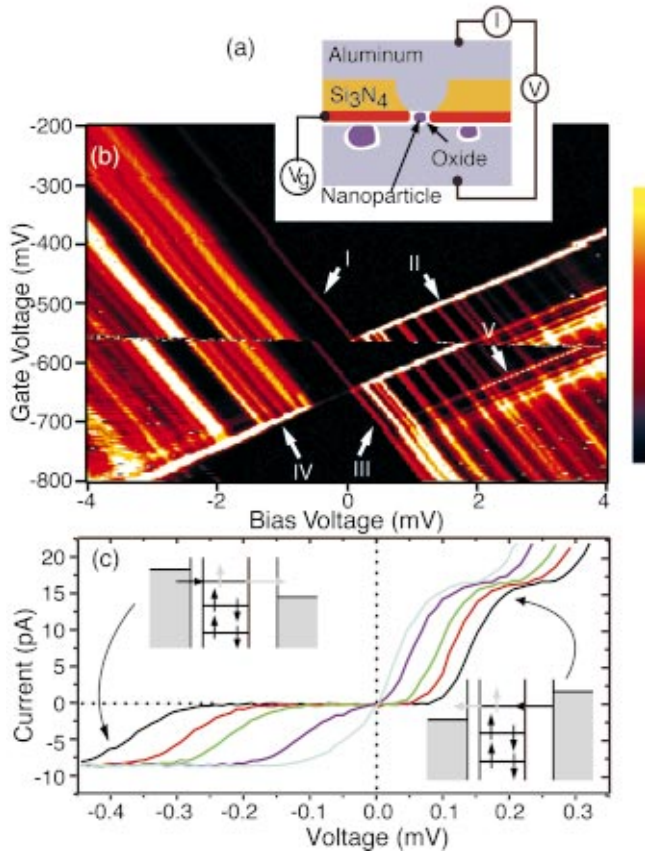


FIG. 1. (Color) (a) Cross-sectional device schematic. (b) Color-scale differential conductance as a function of V_g and V . A 0.06 T field is applied to drive the Al leads normal. The conductance scale maximum is $3 \times 10^{-7} \Omega^{-1}$. (c) I vs V for different V_g in the equilibrium regime. The steps correspond to resonances III and IV. Insets show the corresponding tunneling transitions.

chemical potential in electrode i). Our observations are in excellent accord with this model. For instance, the tunneling current through the quantum state is not the same for both bias directions, being $I_+ = 16.6 \pm 0.1$ pA for $V > 0$ (i.e., crossing lines II or III) and $I_- = -8.4 \pm 0.1$ pA for $V < 0$ (crossing lines I or IV). This has been observed

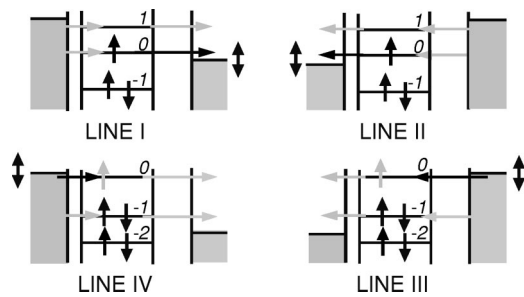


FIG. 2. Tunneling diagrams depicting tunneling transitions active for resonance lines I–IV in a nonequilibrium regime. Black spins represent the ground-state electron configuration. Black arrows indicate the threshold tunneling transition, and gray arrows denote other transitions that contribute to the current for the value of V depicted.

previously^{3,12} and is a consequence of spin degeneracy. For $V > 0$, electrons tunnel across the high-resistance rate-limiting tunnel barrier into an empty state, so that either spin-up or spin-down electrons can tunnel. For $V < 0$, the rate-limiting step is for an electron of a given spin on the particle to tunnel through the high-resistance barrier, and the current level is approximately cut in half. By equating the measured currents to Eq. (1), we determine $\gamma_{0R} = (5.3 \pm 0.1) \times 10^7 \text{ s}^{-1}$ for the high-resistance junction and $\gamma_{0L} \sim 7 \times 10^9 \text{ s}^{-1}$. In addition, for resonances (e.g., III, IV) in which the spin degeneracy of the state is split by a magnetic field, the currents through the two Zeeman states for a given bias direction are not equal,^{7,13} in agreement with the simple tunneling theory. The maximum current through the lower-energy Zeeman state is $e \gamma_{0L} \gamma_{0R} / (\gamma_{0L} + \gamma_{0R})$ for either bias direction, and the second state then adds current to produce the maximum allowed by Eq. (1).

An interesting feature of Eq. (1) when the tunneling threshold is across the lower-resistance barrier (peaks II and IV) is that the maximum of dI/dV does not occur exactly when $\mu_i = \epsilon_0$. Instead, the resonance is shifted to lower $|V|$, by an amount $\propto T$, so that it shifts with T . This is due to charge accumulation on the particle as the Fermi function sweeps by the energy of the quantum state, which limits the current at larger $|V|$ on account of Coulomb blockade. Our observations of this effect (not shown) are equivalent to results of Deshpande *et al.*¹² although the data in Ref. 12 were compared to an approximation that differed from Eq. (1) (Ref. 10).

Nonequilibrium regime: We can controllably tune the device so that more than one quantum state can participate in tunneling. This is illustrated by following line II in Fig. 1(b). This line corresponds to processes that are initiated by an electron, tunneling off the nanoparticle from the quantum state 0 to electrode L . However, as one follows line II to higher V , past negative-sloping resonance lines that intersect line II, these lines indicate that the subsequent tunneling of an electron from electrode R back onto the nanoparticle can proceed via many different energy levels other than state 0. The total current under these conditions can be modeled by a master equation, which takes into account all allowed transitions between the energetically accessible n_0 and $(n_0 - 1)$ electron states.⁹ In Fig. 2, we show tunneling diagrams depicting representative accessible states for resonances I–IV in a nonequilibrium regime.

In Fig. 3(a), we plot the step height in current associated with resonance lines I–IV, as V_g and V are tuned to follow the lines in the $|V|$ - V_g plane. Peaks I and III have approximately constant amplitude, while the currents for peaks II and IV grow quickly as $|V|$ enters the nonequilibrium regime. This can be understood trivially. For peaks I and III, the tunneling threshold is across the higher-resistance tunnel junction R . This junction is always rate limiting and it matters little how many transport channels are available across junction L . For peaks II and IV, the tunneling threshold is across the low-resistance barrier L , but the rate-limiting process is how quickly electrons can tunnel across the other barrier. As $|V|$ is increased, more quantum levels contribute to this process, and the current grows. By measuring the

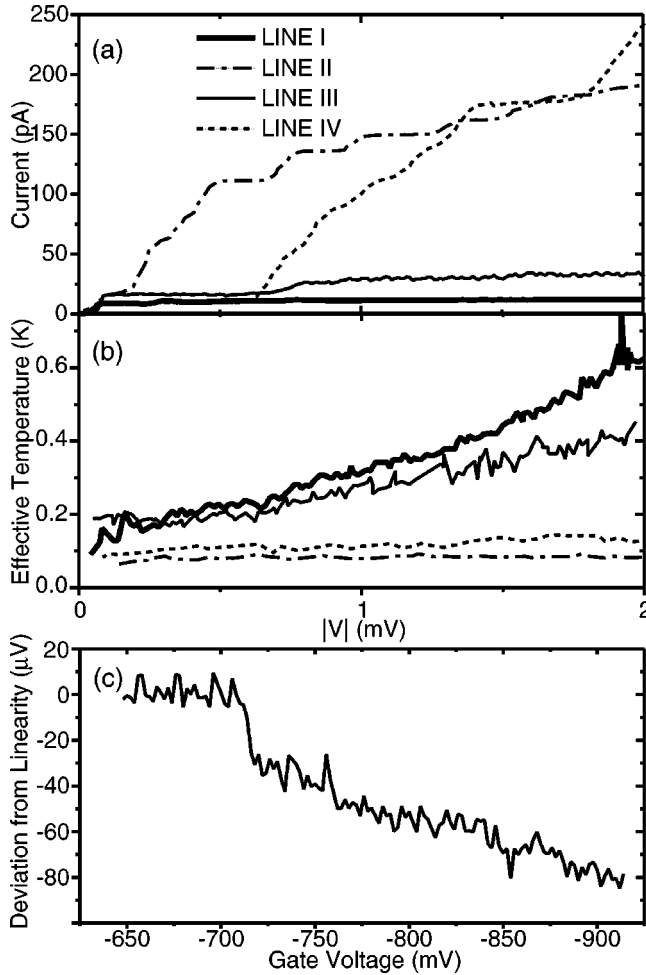


FIG. 3. Properties of the resonance lines as V_g is varied to change the value of the V at which the resonances appear. The second tunneling states become energetically accessible for $|V| > 0.18$ mV for resonance line I, 0.19 for line II, 0.50 mV for line III, and 0.64 mV for line IV. (a) Magnitude of tunneling current. (b) Width of the dI/dV peak as a function of V , expressed as an effective temperature. (c) Deviation from linearity for the V position of peak III as a function of V_g . A line was fit to the peak position in the equilibrium regime between $V_g = -650$ mV and -701 mV, and this was subtracted from the measured positions.

current along peaks II and IV as levels are added one by one, and then fitting to master-equation results,⁹ we can measure rate-limiting tunneling rates for each quantum state: the γ_{iR} , for $i=0$ to 5, are $(5.3, 15.7, 8.0, 16, 15, 9) \times 10^7$ s⁻¹, $\bar{\gamma}_L \approx 3 \times 10^9$ s⁻¹, and (assuming relaxation effects are negligible) $\gamma_{-1R} \approx 17 \times 10^7$ s⁻¹.

Figure 3(b) shows the widths of the tunneling resonance lines I–IV. These were determined by fitting the V dependence of each conductance peak to the derivative of a Fermi function, and then converting the voltage width to effective temperature by multiplying by the capacitance ratio $(e/k_B)C_L/(C_L + C_R)$ for peaks I and III or $(e/k_B)C_R/(C_L + C_R)$ for peaks II and IV (Ref. 7). In either the equilibrium or nonequilibrium regimes, the prediction of the simplest master equation⁹ is that the peak shape should be a derivative of the Fermi function with a width approximately equal to

the electronic temperature in the electrodes. Our measurements agree with this model within the equilibrium regime, with a constant electron temperature $T \approx 90$ mK. This is significantly higher than the T achieved in nongated tunneling devices using our apparatus (45 mK), and we ascribe the difference to heating by leakage current from the gate to electrode R . Line III is broader than the others at low V because the magnetic field of 60 mT applied to drive the Al electrodes normal produces an unresolved Zeeman splitting ($\Delta E/k_B = 2\mu_B H/k_B = 80$ mK).

As $|V|$ is increased into the nonequilibrium regime, peaks I and III undergo large increases in width and peak IV broadens slightly, while peak II shows no measurable change. The differences are not merely an effect of heating, because peaks II and IV have the largest magnitudes of current and power. We suggest that these measurements can be explained as a consequence of electronic interactions in the nonequilibrium regime, by a mechanism due to Agam *et al.*¹⁴ Consider resonance line III, for which the tunneling threshold corresponds to an electron entering quantum state 0. For $V > 0.50$ mV the next tunneling event, which discharges the particle, may occur out of different, lower energy states (see Fig. 2), leaving an electron-hole excitation on the nanoparticle. Agam *et al.* suggested that if this nonequilibrium state does not relax before the next electron tunnels onto the particle, it can shift the energy of the tunneling resonances on account of an alteration of the electron-electron interaction energy.¹⁵ In past work on smaller aluminum particles, shifted transitions were resolved individually;¹⁴ however, the relative shift is expected to decrease with increasing nanoparticle size,¹⁴ so it is reasonable that the shifts would produce only broadened resonances for the 10 nm particle under investigation here. Because a growing ensemble of different nonequilibrium states can be excited with increasing $|V|$, this mechanism can explain the increase in width of line III as a function of $|V|$. The same nonequilibrium mechanisms should also come into play for line IV, for $V < -0.64$ mV, but the broadening here is reduced because the threshold tunneling event is across the lower-resistance junction L . Barrier R quickly becomes rate limiting as line IV is crossed, so that higher-energy nonequilibrium resonances do not add significant additional current. In order for the nonequilibrium mechanism to apply for line III, the relaxation rate of some nonequilibrium excitations to the ground state must be comparable to or slower than $\gamma_{0R} = 5.3 \times 10^7$ s⁻¹. The rate predicted by Agam *et al.* for *spin-preserving* energy relaxation in Al particles is $\sim 10^8$ s⁻¹.¹⁴

Resonances I and II are a different case, because the tunneling threshold corresponds to an electron leaving quantum state 0. The subsequent tunneling event adding an electron back to the nanoparticle may, for large V , occur in higher energy states [see Fig. 2(a,b)], but nevertheless this excitation alone cannot produce a nonequilibrium shift in the energy of subsequent discharging transitions. The reason is that only this electron is free to tunnel off the nanoparticle; there is no electron in quantum state 0 whose transition energy might be shifted. Therefore, within the picture of Agam *et al.*,¹⁴ no nonequilibrium broadening should be expected for levels I and II, in conflict with the data for level I.

This discrepancy can be explained if nonequilibrium excitations on the nanoparticle can be generated not only by the tunneling transitions on or off the particle that have been considered previously,¹⁴ but also by transitions in which a high-energy electron relaxes within the nanoparticle and produces an electron-hole excitation. Broadening would then be generated by the Agam mechanism. Within this scenario, the difference between the broadening visible for resonance line I and the lack of broadening of line II would follow from the fact that for peak II a high-energy electron on the particle can quickly exit through the low-resistance tunnel junction L , while for peak I the high-energy particle must exit through the high-resistance junction R , giving a much longer residence time during which relaxation transitions can occur. In order for line I to be broadened, the fastest relaxation rates must become comparable to $\gamma_{0R} = 5.3 \times 10^7 \text{ s}^{-1}$ as $|V|$ increases.

By tuning V_g and V into the nonequilibrium regime, the apparent *energies* of the dI/dV peaks can also be changed. This is clearest for line III [Fig. 3(c)], which undergoes a shift of $33 \text{ } \mu\text{V}$ to lower voltage when the threshold for nonequilibrium tunneling via state -1 [line V in Fig. 1(b)] is crossed. Because we have measured rate-limiting tunneling rates for the energetically accessible states from the current amplitudes, we can test whether this shift can be explained by the simplest master equation,⁹ which assumes that the underlying energies of the quantum states are not changed by nonequilibrium interactions. Only one relevant parameter is not determined previously: $x = \gamma_{0L}/\gamma_{-1L}$. The solution of the master equation does predict a voltage shift ($\propto T$) for the conductance peak compared to the equilibrium case, and for $x < 0.15$ it can explain the full value of the experimental shift. However, we judge this to be improbable, because the measured values of γ_{iR} fall within a more narrow distribution. For $x \sim 1$ in Eq. (2), the predicted shift is

$15 \text{ } \mu\text{V}$ —much smaller than we measure. We can more naturally explain the full value of the shift by again taking into account that the presence of a nonequilibrium excitation can change the energy of a tunneling transition. In the equilibrium regime, the occupation of quantum state 0 corresponds to a transition from a fully paired superconducting state on the aluminum particle to a state with one high-energy quasiparticle; in the nonequilibrium case, the transition can be from a state with two quasiparticles to one, with a transition energy lowered by $\sim 2\Delta \approx 0.35 \text{ meV}$.¹⁶ This is much bigger than $k_B T \sim 10 \text{ } \mu\text{eV}$, and in this case the observed resonance is shifted to lower $|V|$ by an amount $\propto T$ because electrons in the tail of the Fermi distribution can excite the nonequilibrium state and open the lower-energy current channel.⁹ For $x = 1$ and $T \sim 90 \text{ mK}$ the master-equation result⁹ is that the measured shift can be produced by a nonequilibrium lowering of the transition energy by any amount greater than $20 \text{ } \mu\text{eV} \sim 2k_B T$.

In summary, we have made a systematic study of the fundamental processes at work when electrons undergo tunneling through a discrete-state system, by analyzing the resonance energies, widths, and current levels. When transport occurs through a single level, our results are in agreement with the expectations of sequential tunneling. At large values of $|V|$, the nonequilibrium population of excited electronic states, together with electron-electron interactions, modifies the widths of the tunneling resonances and causes their apparent energies to shift as a function of temperature. Our results should apply to any nanometer-scale system in which electrons tunnel sequentially through well-resolved states.

ACKNOWLEDGMENTS

Support from NSF DMR-0071631, the Packard Foundation, and the Cornell Nanofabrication Facility are acknowledged.

¹R.C. Ashoori, *Nature* (London) **379**, 413 (1996).

²J. von Delft and D.C. Ralph, *Phys. Rep.* **345**, 61 (2001).

³D.H. Cobden *et al.*, *Phys. Rev. Lett.* **81**, 681 (1998).

⁴D.C. Ralph, C.T. Black, and M. Tinkham, *Phys. Rev. Lett.* **78**, 4087 (1997).

⁵C. T. Black, Ph.D. thesis, Harvard University, 1996.

⁶J.G. Lu, J.M. Hergenrother, and M. Tinkham, *Phys. Rev. B* **57**, 4591 (1998).

⁷D.C. Ralph, C.T. Black, and M. Tinkham, *Phys. Rev. Lett.* **74**, 3241 (1995).

⁸L.I. Glazman and K.A. Matveev, *JETP Lett.* **48**, 445 (1988).

⁹E. Bonet, M.M. Deshmukh, and D.C. Ralph, *Phys. Rev. B* (to be published); cond-mat/0108248.

¹⁰Equation 1 differs from the analysis in Refs. 12,13. M. R. Deshpande agrees that their equations were an approximation.

¹¹In the case where one quantum level is either singly or doubly occupied, the sequential tunneling current is

$$I = e \frac{2\gamma_{0L}\gamma_{0R}(f_L - f_R)}{(2 - f_L)\gamma_{0L} + (2 - f_R)\gamma_{0R}}. \quad (2)$$

¹²M.R. Deshpande, J.W. Sleight, M.A. Reed, and R.G. Wheeler, *Phys. Rev. B* **62**, 8240 (2000).

¹³M.R. Deshpande *et al.*, *Phys. Rev. Lett.* **76**, 1328 (1996).

¹⁴O. Agam *et al.*, *Phys. Rev. Lett.* **78**, 1956 (1997).

¹⁵A statement in Ref. 14 that the first tunneling resonance should be unaffected by nonequilibrium is incorrect in some cases when spin is taken into account.

¹⁶M. Schechter and J. von Delft (private communication).